American Mineralogist, Volume 67, pages 14–27, 1982

Mineralogy of mafic and Fe–Ti oxide-rich differentiates of the Marcy anorthosite massif, Adirondacks, New York

LEWIS D. ASHWAL

Lunar and Planetary Institute
3303 NASA Road 1, Houston, Texas 77058

Abstract

Rocks enriched in mafic silicates, Fe–Ti oxides and apatite form a minor but ubiquitous facies of nearly all Proterozoic massif-type anorthosite complexes. In the Marcy massif of the Adirondack highlands, New York, the mafic rocks have two modes of occurrence: 1) as conformable segregations interpreted as cumulate layers in the border zones, and 2) as dikes throughout the massif, interpreted as having crystallized from residual liquids extracted at varying stages during differentiation. Primary mineral compositions in these rocks are commonly preserved, despite the effects of subsolidus recrystallization in the high pressure granulite facies. In the mafic rock suite, primary compositions of mafic silicates reveal an iron enrichment trend which is broadly similar to that of basic layered intrusions, but suggestive of somewhat higher crystallization temperatures. Textural relationships suggest the following crystallization sequence: plagioclase, pigeonite + augite, hemo-ilmenite + magnetite, apatite. Fe-rich olivine replaced pigeonite in the latest-stage residual liquids. The mineralogy and field relationships of these mafic rocks are consistent with their origin as differentiates from the same melts which produced the anorthosites. This conclusion agrees with recent geochemical data that suggest an independent origin for the spatially associated mangerite–charnockite suite.

Introduction

For the past several decades, the controversy over the origin of massif-type anorthosites has centered around the question of the consanguinity of anorthositic rocks and spatially associated suites of orthopyroxene-bearing granitic rocks (charnockite–mangerite series). Recent trace element geochemical studies focusing on, but not limited to, rare earth elements (REE) (Philpotts *et al.*, 1966; Green *et al.*, 1969, 1972; Seifert *et al.*, 1977; Seifert, 1978; Simmons and Hanson, 1978; Ashwal and Seifert, 1980) demonstrate that the acidic rocks do not represent differentiates from the melts which produced the anorthosites. This was recognized as early as 1939 by A. F. Buddington on the basis of field relationships (summarized by Buddington, 1969).

In addition to huge volumes of pure anorthosite, the typical massif anorthosite *suite* contains minor facies with larger proportions of mafic silicates, Fe–Ti oxides and apatite. Extreme concentrations of these minerals give rise to minor ultramafic rocks, as well as the ilmenite–magnetite ore deposits whose association with anorthosite massifs is well known (Rose, 1969). It is these mafic rocks, and not the mangerite–charnockites, which complement the anorthosites, as demonstrated by REE geochemical relationships (Ashwal and Seifert, 1980). The purpose of this paper is to describe the field relationships and mineralogical characteristics of mafic rocks associated with the Marcy anorthosite massif in the Adirondack highlands of northern New York State, and to emphasize the importance of these rocks in understanding the fractionation histories of this and other massif-type anorthosite complexes.

Field relations of mafic facies of anorthosite

In the Marcy massif, the most felsic anorthosites are found in the central regions, and more mafic varieties occur near the margins. Because of the domical form of the massif, the mafic border facies overlies the anorthositic core zone (Buddington, 1939, 1960, 1969). In some places there is a systematic increase in mafic silicates and oxide minerals from coarse, core zone anorthosite (Marcy facies) structurally upwards to finer-grained, border zone

0003–004X/82/0102–0014$02.00

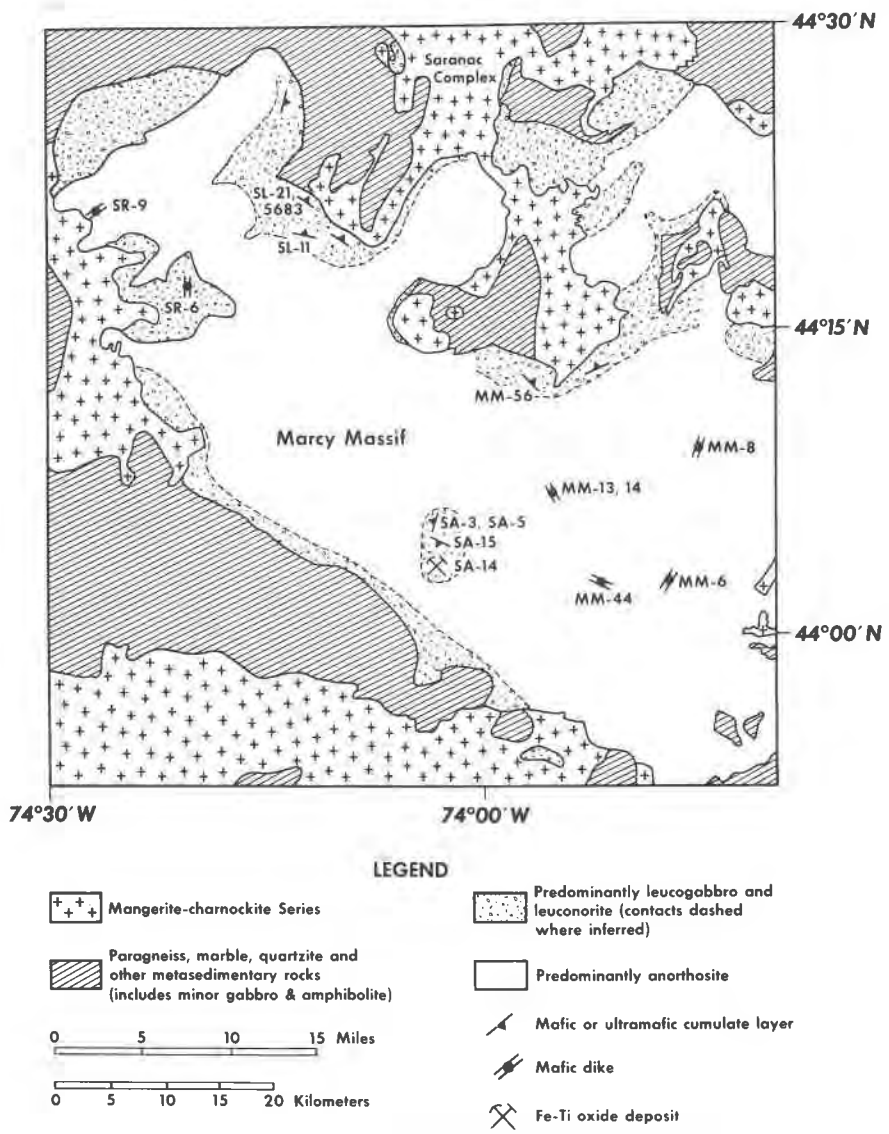

Fig. 1 Geologic map of the Marcy anorthosite massif, Adirondacks, New York, showing sample locations. Base map taken from Isachsen and Fisher (1970).

gabbroic anorthosite[1] (Whiteface facies) (Buddington, 1939; Davis, 1971). Elsewhere, the border zones contain local mafic to ultramafic layers (color index > 40%) which are conformable to foliation in host gabbroic anorthosites. Mafic rocks also occur as dikes throughout the massif, as discussed below. The distribution and structural relationships, where known, of these mafic layers and dikes are shown on a geologic map of the Marcy massif in Figure 1.[2]

In the border zones, local ultramafic layers commonly have sharp lower contacts and are gradational upwards into more feldspathic rocks. These are most easily interpreted as resulting from processes involving gravitational settling and accumulation of mafic silicates and Fe–Ti oxide minerals. The layers range in thickness from 1 cm to 1 m and are often

[1]Rocks are classified on the basis of color index (volume % mafic minerals), and the mineralogical modifiers *gabbroic, noritic*, or *troctolitic* are used depending on whether the predominant mafic phase is high-Ca pyroxene, low-Ca pyroxene, or olivine, respectively (Buddington, 1939; Streckeisen, 1976). The modifier *oxide-rich* is added when modal ilmenite + magnetite exceeds 10%.

[2]Details of sample locations may be obtained by ordering Document AM-82-182 from the Business Office, Mineralogical Society of America, 2000 Florida Avenue, N.W., Washington, D.C. 20009. Please remit $1.00 in advance for the microfiche.

rhythmically repeated several times on the scale of individual outcrops. The attitudes of the layers are in most places consistent with the domical shape of the massifs (Fig. 1), although their lateral extent is difficult to estimate due to the paucity of exposures.

There are also mafic rocks which occur as sharp-walled dikes of varied composition, crosscutting the anorthositic foliation at high angles. These dikes may have crystallized from residual liquids extracted at various stages of differentiation of the anorthosite suite (Ashwal, 1978a, b). In the Marcy massif, mafic dikes are not spatially restricted to the border facies, but may be found even in the central regions (Fig. 1). The dikes are generally less than 7 m thick, although Buddington (1939, p. 50–51) described a mafic gabbro dike some 60 m wide in the Carthage anorthosite massif in the western Adirondacks.

Mineral constitution and petrography

Primary minerals of the Marcy anorthosite complex include plagioclase, high-Ca pyroxene, low-Ca pyroxene, olivine, ferrian ilmenite, titaniferous magnetite, and apatite. Metamorphic minerals include garnet, hornblende, biotite and quartz, in addition to recrystallized equivalents of the primary phases, suggesting equilibration in the high pressure granulite facies (deWaard, 1965).

Conformable occurrences of mafic rocks

Modes of conformable mafic facies rocks from the Marcy massif are given in Table 1. There is generally a progressive decrease in mafic and oxide minerals with increasing stratigraphic height above the basal contact of a cumulate layer; the scale over which this variation in modal mineralogy takes place ranges from centimeters to meters. Cumulus phases include augite, inverted pigeonite, ilmenite, magnetite, and, less commonly, Fe-rich olivine and apatite. The primary mineralogies and textures of these rocks, however, have been affected to varying degrees by subsolidus recrystallization, which has resulted in the production of metamorphic garnet and hornblende, and in the reconstitution of coarsely exsolved pyroxenes into smaller discrete grains with different compositions. Zones of garnet 1–5 mm thick commonly occur between the basal contacts of mafic layers and underlying leucogabbros or leuconorites. Although metamorphic garnet, hornblende, and pyroxenes constitute nearly 20% of some samples, other rocks appear to have completely retained their primary mineralogies and textures (Table 1, sample SA-3D). In general, it is possible to see through the overprinting effects of subsolidus recrystallization, as discussed below.

The color indices of the lower, most mafic parts of the layers vary between approximately 60% and 100% (Table 1). The layers generally lie on and are

Table 1. Point counted modes of conformable mafic rich rocks from the Marcy massif

	SA-3D	SA-3A	SA-5	SL-11Y	SL-11A	SA-15A	SA-15B	MM-56B	MM-56A	SL-21A	SL-21	5683d
Plagioclase	1.2*	63.7	66.8	2.8	75.6*	42.6*	73.5*	20.9	74.0*	19.3*	51.5*	27.1*
Inverted pigeonite	22.4	9.5	21.7	4.7	tr	7.1	3.2	1.7	-	-	-	tr
Orthopyroxene	-	3.2	2.4	7.1	3.4	4.8	2.1	7.0	3.6	0.9	1.9	-
Clinopyroxene	36.4	9.9	4.1	52.3	13.4	19.0	11.4	28.9	11.2	48.6	16.6	9.5
Olivine	-	-	-	-	-	-	-	-	-	-	-	21.4
Ilmenite	25.6	1.1	0.9	18.9	4.5	12.3	5.9	15.3	4.2	4.3	11.7	8.4
Magnetite	13.9**	0.6	0.1	4.2	0.3	1.3	0.1	1.0	0.7	16.2		3.3
Apatite	-	0.2	-	-	0.2	0.5	-	-	0.6	8.6	2.6	7.1
Garnet	-	11.5	3.7	-	2.2	12.2	3.2	10.5	4.7	1.1	15.2	18.0
Hornblende	-	-	0.2	9.0	-	-	-	14.7	0.5	-	-	-
Sulfides	0.5	-	0.1	1.0	0.2	-	0.2	-	-	-	-	-
Biotite	tr	-	-	-	-	0.2	0.4	-	-	0.5	-	4.7
Scapolite	-	0.3	-	-	-	-	-	-	-	-	-	-
Other secondaries***	-	tr	-	-	0.2	-	-	-	0.5	0.5	0.5	0.5
	100.0	100.0	100.0	100.0	100.0	100.0	100.0	100.0	100.0	100.0	100.0	100.0
Color index	98.8	36.3	33.2	97.2	24.4	57.4	26.5	79.1	26.0	80.7	48.0	72.9
	oxide-rich pyroxenite layer	leuconorite host	leuconorite host	oxide-rich pyroxenite layer	leuconorite host	oxide-rich gabbro layer	leucogabbro host	oxide-rich mafic gabbro layer	leucogabbro host	oxide-rich mafic gabbro layer	oxide-rich gabbro host	oxide-rich mafic troctolite layer

* includes minor antiperthite; ** includes trace amount of pleonaste; *** includes sericite and hematite alteration

gradational structurally upwards into host rocks of leucogabbroic or leuconoritic composition (color index 26% to 36%), although in some cases the host rock has a color index as high as 46% (Table 1, sample SL-21).

In all layers, high-Ca pyroxene (augite) dominates over low-Ca pyroxene (inverted pigeonite and/or orthopyroxene). The large high-Ca/low-Ca pyroxene ratio in the highly recrystallized rocks (*e.g.*, MM-56B) may be due to the increase in discrete augite grains from the recrystallization of coarsely exsolved primary pyroxenes. The paucity of low-Ca pyroxene in other specimens (*e.g.*, SL-21, SL-21A, 5683d) is related to the onset of Fe-rich olivine crystallization, which replaced low-Ca pyroxene during the later stages of solidification. Olivine-bearing layers such as represented by specimen 5683d do, however, contain minor inverted pigeonite. The low-Ca pyroxene-deficient or olivine-bearing layers, or both, contain abundant apatite, which also must be a late-stage cumulus phase. In addition to their mineralogy, the location of these layers at the extreme margins of the massifs (Fig. 1), and hence at the highest stratigraphic levels, suggests that they may represent some of the very last accumulations from late stage mafic liquids which had been segregated to the upper regions of the massifs.

All of the conformable mafic layers contain major amounts (>10%) of ilmenite and magnetite. In some cases, the oxide mineral content is sufficiently high that the rock can be considered ore grade. Conformable oxide mineral-rich layers within gabbro or leucogabbro are particularly abundant in the Sanford Lake area where they are mined for their ilmenite concentrations (Gross, 1968), but similar layers of much lesser extent have been reported from elsewhere in the Marcy massif (Buddington, 1953, Table 1, sample no. 20). Ilmenite usually predominates over magnetite in the conformable layers, although there are examples where the reverse is true (Table 1, sample SL-21A).

Mafic dikes

Modes of mafic dikes from the Marcy massif are given in Table 2. The dikes show wide ranges in color index (approximately 40–90%), and mineral constitutions. It is important to determine which, if any, of these dike rocks represent liquids. They are finer grained than the mafic cumulate rocks; however, primary textures in the dike rocks are generally not well preserved. Many contain abundant garnet (Table 2). The profound effect of garnet production on modal mineralogy (particularly color index) may be seen by comparing the modes of samples SR-9 and MM-6 (Table 2), which despite their large

Table 2. Point counted modes of mafic rich dikes from the Marcy massif

	MM-8	MM-14A	MM-13A	SR-6	SA-14A	MM-6	SR-9	MM-44A
Plagioclase	8.0	33.8*	45.6*	42.3	43.2	26.8	50.0*	0.4
Inverted pigeonite	-	22.5	0.9	-	-	-	-	-
Orthopyroxene	63.4	1.9	10.8	6.4	3.1	-	-	-
Clinopyroxene	23.7	12.2	17.7	14.3	24.7	17.5	17.0	23.3
Olivine**	-	-	-	-	-	14.4	9.7	42.1
Ilmenite	3.0	10.9	8.7	7.2	11.1	10.1	6.8	13.1
Magnetite		2.6	3.1		2.7	3.9	5.8	9.2
Apatite	-	5.4	4.7	2.3	0.5	5.7	4.3	6.0
Garnet	-	9.1	8.4	23.9	4.1	19.7	6.4	4.4
Hornblende	1.9	1.6	-	-	10.2	-	-	-
Sulfides	-	-	0.1	-	0.4	-	tr	-
Other secondaries***	-	-	-	3.6	-	1.9	-	1.5
	100.0	100.0	100.0	100.0	100.0	100.0	100.0	100.0
Color index	92.0	66.2	54.4	54.1	56.8	71.3	50.0	98.1
Rock type	pyroxenite	oxide-rich mafic norite	oxide-rich gabbro	gabbro	oxide-rich gabbro	oxide-rich mafic gabbro	oxide-rich gabbro	oxide-rich wehrlite

* includes minor antiperthite; ** includes iddingsite alteration; *** includes sericite and hematite alteration

mineralogical differences, have similar bulk compositions. Thin layers of garnet are also found at the contacts between some of the dikes and the surrounding anorthositic rocks in a manner similar to that of the garnet zones at the basal contacts of the ultramafic cumulates. Because of these garnet zones, it is impossible to determine whether these dikes once had chilled margins.

Oxide-rich, olivine gabbro or mafic gabbro dikes which lack low-Ca pyroxene (samples SR-9 and MM-6, Table 2) may have crystallized from the final liquid differentiates of the anorthosite suite, since their REE patterns (Ashwal and Seifert, 1980) are characterized by high total abundances and negative Eu anomalies, and relative light REE depletion. These patterns are complementary to anorthosites and leucogabbros, which exhibit low REE abundances, positive Eu anomalies, and relative light REE enrichment (Seifert *et al.*, 1977; Simmons and Hanson, 1978). Mineral compositions of these dikes are consistent with their origin as latest-stage differentiates, as discussed below.

Although the mafic dikes probably in large part represent liquid compositions, the possibility of mineral accumulation or loss in these liquids during or after their emplacement as dikes must be considered. Additionally, there are rare examples of ultramafic dikes including hypersthenite (sample MM-8) and oxide-rich wehrlite (sample MM-44A) which may represent remobilized cumulates (deWaard, 1970). These complications must be taken into account before accurate liquid lines of descent can be determined.

Petrographic determination of crystallization sequence

Despite the effects of subsolidus recrystallization, primary igneous textures are preserved in many cases, permitting the distinction of cumulus and post-cumulus phases and allowing the determination of crystallization sequences. Plagioclase in the Marcy massif and in other anorthosite complexes was the first phase to crystallize. Evidence for this conclusion includes large, euhedral or subhedral plagioclase crystals with smaller, anhedral pyroxenes in interstitial areas. A common feature of anorthositic rocks in the central parts of massifs is the alignment of tabular plagioclase crystals with their longest dimensions subparallel, forming a planar fabric in the rock. The implication of this texture is that the anorthosites represent *accumulations* of plagioclase concentrated either gravitationally or by flowage (Emslie, 1975; Martignole, 1974; Morse, 1969; Olmstead, 1969).

Primary textures suggest that the pyroxenes crystallized after plagioclase, and in turn were followed by the Fe–Ti oxide minerals. It is not possible on textural grounds to determine whether augite or pigeonite crystallized first, but it is likely that they precipitated simultaneously during most of the crystallization history. In the anorthosites, leucogabbros, and leuconorites, coarsely exsolved primary pyroxenes or their metamorphic equivalents partially surround earlier and larger plagioclase crystals in a subophitic relationship. More mafic rocks also have subophitic textures; however, the presence of large, discrete pyroxene crystals of probable cumulate origin suggest co-crystallization of plagioclase and pyroxene. In contrast to the tabular shape of plagioclase, cumulus mafic silicates are equant in shape, and the ultramafic cumulates (oxide-rich pyroxenites) have an equigranular texture.

In a similar manner, ilmenite and magnetite partially or completely surround the pyroxenes, suggesting that the oxides crystallized later, and this texture is particularly well developed in the oxide-rich pyroxenite cumulate layers. The oxide minerals may constitute up to 40% of these rocks (Table 1), and since the layers grade structurally upwards into less oxide-rich rocks, the textures may be interpreted to represent cumulus Fe–Ti oxides which have been extended interstitially by post-cumulus growth. Oxide rich pyroxenite layers with similar textures have been reported from other anorthosite massifs (Subramaniam, 1956, Fig. 3) and are also present in zoned ultramafic complexes (Taylor and Noble, 1969, Fig. 10).

Apatite occurs as a cumulus phase only in the very late-stage low-Ca pyroxene-deficient or olivine-bearing cumulates, or both. In these rocks it occurs as intergrowths with the Fe–Ti oxides, although aggregates of very coarse apatite crystals (up to 1 mm across) are also found. Olivine occurs as large cumulus grains up to 5 mm across which, in some cases, poikilitically enclose pyroxenes, apatite and plagioclase; it also occurs as smaller, rounded grains within cumulus augite crystals (sample 5683d). Sparse grains of inverted pigeonite are invariably present in this layer, which represents the only known coexistence of three primary mafic silicates in the Marcy massif.

Mineral compositions

Pyroxenes and olivines

All primary minerals in the anorthosite–mafic gabbro suite with the exception of olivine and apatite contain complex subsolidus exsolution features. Primary pyroxene compositions, however, can be reasonably ascertained by bulk analysis using broad-beam electron microprobe techniques. This has been done for pyroxenes of the Adirondack Marcy massif using a combination of energy dispersive (ED) and wavelength dispersive (WD) microprobe techniques.[3]

In the Marcy massif, many low-Ca pyroxenes contain broad exsolution lamellae of augite inclined to the (001) directions of the present orthopyroxene hosts, and later fine augite lamellae parallel to (100) of their hosts (Fig. 2a). These textures suggest initial crystallization of pigeonite, followed by exsolution and inversion to orthopyroxene in response to slow cooling. Coexisting augites commonly contain several generations of pigeonite lamellae, as described in detail by Jaffe *et al.* (1975).

Primary compositions of coexisting augite-inverted pigeonite and augite–olivine pairs from mafic cumulate layers and dikes are plotted in Figure 3a. Representative ED and WD microprobe analyses for one sample are given in Table 3.[4] The compositions show a wide range in fe* [molar Fe/(Fe+Mg)], and define a fractionation trend which is broadly similar to that of basic layered intrusions. In the Marcy massif, however, the coexisting pyroxenes are consistent with a narrower solvus, and may reflect higher initial crystallization temperatures than those of the Skaergaard intrusion (Fig. 3).

The coexisting mafic silicates from cumulate layers define a trend of increasing fe* with increasing stratigraphic height. For example, sample SA-3D, an oxide-rich pyroxenite layer, contains the most magnesian augite-inverted pigeonite pair yet found in the Marcy massif (fe* of low-Ca pyroxene = 0.36). Samples SA-3A and SA-5 are more feldspathic leuconorites which are conformable with, and occur within a few meters stratigraphically

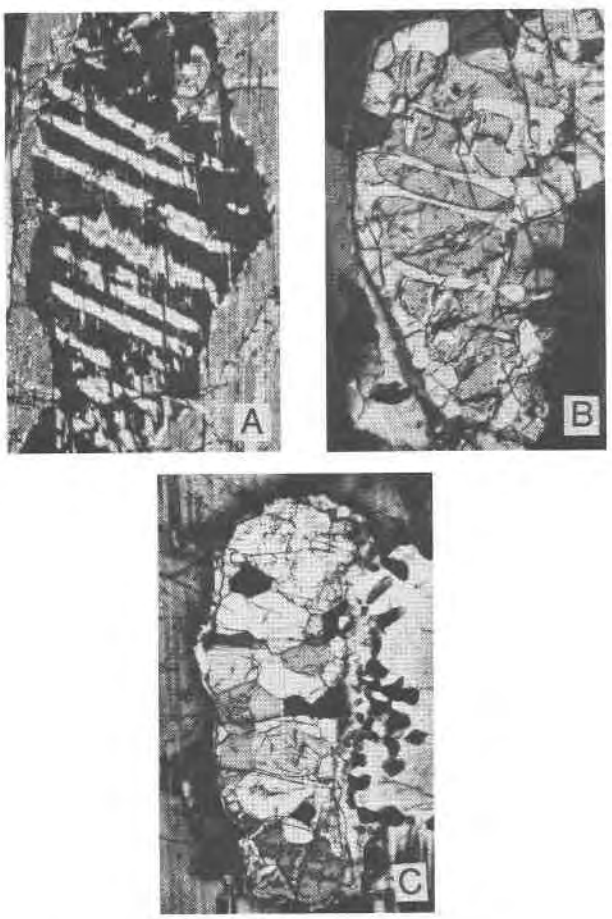

Fig. 2. Photomicrographs illustrating progressive recrystallization of primary pyroxenes (crossed nicols). (A): Primary inverted pigeonite surrounded by primary augite. Coarse augite lamellae (white) are inclined to the (001) direction of host orthopyroxene (at extinction). A later set of fine (100) augite lamellae (nearly vertical) is also present. Length of photograph: 1 mm. (B): Partially recrystallized inverted pigeonite illustrating the migration and coalesccence of coarse augite lamellae at grain boundaries. Length of photograph: 1.5 mm. (C): Granular mosaic of augite and orthopyroxene illustrating final result of recrystallization. Length of photograph: 2mm.

[3]Primary compositions of coarsely exsolved pyroxenes were determined using an ED microprobe technique, whereby the electron beam was broadened, in some cases up to 100 microns, in order to incorporate entire grains. This method is successful for major elements; ED analyses of host and lamella phases are generally within 5 relative % of WD analyses, and calculated ratios of mineral molecules show excellent agreement (Table 3). However, the poor system resolution and low peak/background ratios make quantitative ED determination of minor element oxides essentially impossible, as illustrated by comparison of values for MnO by WD and ED techniques (Table 3). Because of this, primary pyroxene compositions were determined by re-integrating fine-beam WD analyses of host and lamella phases in the proportions given by the ED analyses in terms of Wo, En and Fs (Table 3).

[4]A complete table of pyroxene and olivine microprobe analyses may be obtained by ordering Document AM-82-183 from the Business Office, Mineralogical Society of America, 2000 Florida Avenue, N.W., Washington, D.C. 20009. Please remit $1.00 in advance for the microfiche.

Table 3. Representative microprobe analyses of pyroxene and olivine from sample 5683d

	Meta. opx.†	Meta. opx.§	Meta. cpx.†	Meta. cpx.§	Primary pig**	Primary cpx.†	Olivine†
SiO_2	51.03	50.6	50.92	51.8	51.00	51.18	32.53
TiO_2	0.11	na	0.34	na	0.17	0.27	na
Al_2O_3	1.38	2.6	3.06	4.2	1.81	2.80	0.00
Cr_2O_3	0.05	na	0.00	na	0.04	0.00	na
FeO*	30.59	29.6	13.79	13.2	26.27	17.29	52.50
MnO	0.45	0.6	0.21	0.1	0.39	0.28	0.44
MgO	16.73	16.0	11.01	11.3	15.26	11.98	14.96
CaO	0.55	0.6	19.84	19.4	5.51	16.12	0.01
Na_2O	0.00	na	0.77	na	0.20	0.77	na
Total	100.89	100.0	99.94	100.0	100.65	100.69	100.44
Structural Formula based on 6 oxygens (pyroxene) or 4 oxygens (olivine)							
Si	1.960	1.952	1.935	1.946	1.953	1.940	0.988
Al^{iv}	0.040	0.048	0.065	0.054	0.047	0.060	0.000
	2.000	2.000	2.000	2.000	2.000	2.000	0.988
Al^{vi}	0.022	0.072	0.072	0.134	0.035	0.065	-
Ti	0.003	-	0.010	-	0.005	0.008	-
Cr	0.002	-	0.000	-	0.001	0.000	-
Fe*	0.983	0.950	0.438	0.414	0.841	0.548	1.334
Mn	0.015	0.021	0.007	0.002	0.013	0.009	0.011
Mg	0.958	0.919	0.624	0.633	0.871	0.677	0.678
Ca	0.023	0.026	0.808	0.778	0.226	0.655	0.000
Na	0.000	-	0.057	-	0.015	0.057	-
	2.006	1.988	2.016	1.961	2.007	2.019	2.023
Wo	1.2	1.4	43.2	42.6	11.7	34.8	
En(Fo)	48.8	48.5	33.4	34.7	45.0	36.0	(33.7)
Fs(Fa)	50.0	50.0	23.4	22.7	43.3	29.2	(66.3)

na not analyzed for; * total Fe as FeO; ** composition of primary inverted pigeonite calculated by combining WDA analyses of host and lamella in proportions given by broad beam EDA analyses; † wavelength dispersive analysis (WDA); § energy dispersive analysis normalized to 100% for comparison with WD analysis

above, this ultramafic cumulate layer, and contain progressively more Fe-rich pyroxene compositions with increasing distance above the basal contact (Fig. 3a). On a larger scale, sample 5683d, a mafic cumulate layer from near the outer margin of the massif (Fig. 1), contains Fe-rich olivine in addition to augite and inverted pigeonite. The compositions of these phases are consistent with the idea previously discussed that this sample may represent an accumulation of mafic crystals from very late-stage liquid. The mineral assemblage in this rock represents the last appearance of low-Ca pyroxene (inverted pigeonite), which had apparently reacted with the liquid to form Fe-rich olivine.

Coexisting augites and olivines from mafic dikes SR-9 and MM-6 are among the most Fe-rich mafic silicates of anorthosite suite rocks. Their compositions are consistent with the hypothesis that these dikes crystallized from the latest-stage residual liquids of the anorthosite suite.

With increasing degrees of metamorphic recrystallization, the pyroxene textures and compositions change in a regular fashion. Augites become progressively more calcic as they are transformed, by means of exsolution of low-Ca pyroxene and accompanying recrystallization, from coarse, primary crystals into finer grained aggregates with mosaic texture (Fig. 2). For the low-Ca pyroxenes, the coarse augite lamellae, originally exsolved parallel to the (001) directions of host pigeonites (Fig. 2a), have gradually migrated to the borders of the grains, where they have coalesced into polygonal aggregates (Fig. 2b). The final result of this process is a fine-grained, granular mosaic of hypersthene and augite (Fig. 2c) whose compositions correspond to those of the host and lamellar phases, respectively, of the original primary grains. Tie-lines joining these metamorphic augites and orthopyroxenes have a shallower slope than those joining the primary augite–pigeonite pairs (Fig. 3b), con-

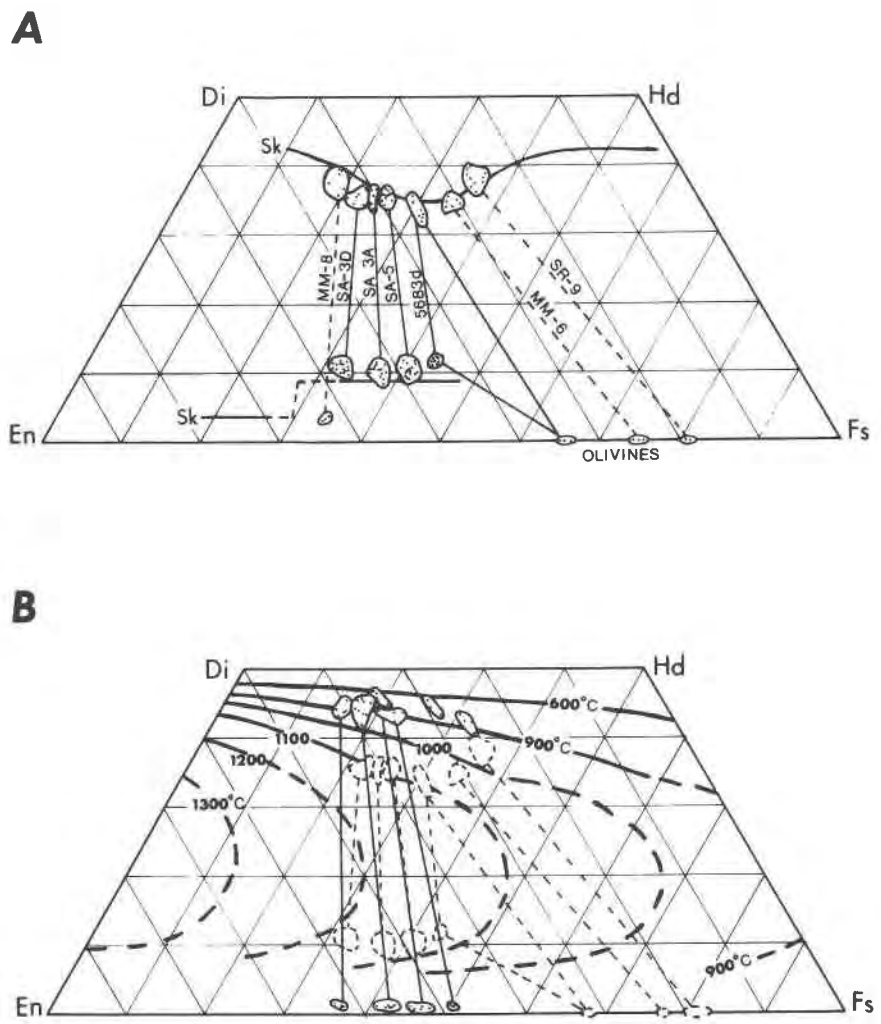

Fig. 3 (A) Primary pyroxene compositions as determined using broad beam energy dispersive techniques, and olivine compositions as determined using wavelength dispersive analyses. Solid tie lines: mafic cumulate layers. Dashed tie lines: mafic dikes. Skaergaard trend after Wager and Brown (1968). (B) Compositions of primary igneous pyroxene and pyroxene–olivine pairs (short dashed lines) and reconstituted metamorphic pairs (solid lines) plotted with respect to the augite–pigeonite solvus (dashed contours) and the augite orthopyroxene solvus (solid contours) of Ross and Huebner (1975).

sistent with the higher $K_D = (Fe/Mg)_{low\text{-}Ca\ pyroxene}/(Fe/Mg)_{high\text{-}Ca\ pyroxene}$ values of metamorphically re-equilibrated pyroxenes (Kretz, 1963). When applied to the pyroxene solvus of Ross and Huebner (1975), the igneous pyroxene pairs yield temperatures in excess of 1100° C, whereas the metamorphic pairs yield temperatures between 600° C and 900° C (Fig. 3b). Both igneous and metamorphic temperatures must, however, be considered as minimum values because of the uncertain effects of increased pressure on the pyroxene solvus. Similar relationships for pyroxenes from the Marcy massif have been reported by Bohlen and Essene (1978).

Plagioclase

Plagioclase in anorthositic rocks from most massif-type complexes generally ranges in composition from An_{40} to An_{65} (mole %) (Anderson, 1969). Because of the extremely large grain size and the rather irregular distribution of exsolved antiperthitic lamellae, the primary compositions of anorthositic plagioclases are difficult to determine, particularly by microprobe analysis. For the Marcy massif, however, Isachsen and Moxham (1969) have analyzed bulk megacryst compositions from two extensive vertical sections using spectrographic meth-

ods. Their measured compositional range among 45 specimens analyzed was $An_{42.6}$ to $An_{55.2}$ and $Or_{1.7}$ to $Or_{10.6}$, with average values of $An_{49.7}$ and $Or_{5.2}$. (These values, given in mole % were converted from the weight percentages reported by Isachsen and Moxham, 1969.) The high K content of anorthositic plagioclase is in accordance with relatively high temperatures of crystallization (Sen, 1959), but precipitation of high-K plagioclase from melts richer in K than typical unfractionated basalts must also be considered as a possibility (Morse, 1981; Ranson, 1981).

In addition to antiperthitic lamellae, anorthositic plagioclases commonly contain minute rodlets and particles of Fe–Ti oxide minerals, also thought to have originated by means of exsolution (Anderson, 1966). Minor element analyses of plagioclase concentrates containing these oxide inclusions (Isachsen and Moxham, 1969) reveal substantial amounts of Fe and Ti (wt.% FeO = 0.27–1.48, avg. = 0.51; wt.% TiO_2 = 0.04–0.85, avg. = 0.28), consistent either with high crystallization temperatures (Smith, 1975), or with high contents of Fe and Ti in the parental magma.

In the mafic rocks, the determination of primary plagioclase composition is further complicated by the presence of abundant garnet, which formed by means of a subsolidus reaction involving a net consumption of anorthite component (McLelland and Whitney, 1977). In many cases this resulted in strongly zoned plagioclase, enriched in albite and orthoclase components towards the garnet. For example, microprobe analyses of plagioclase in oxide-rich mafic gabbro dike MM-6 yield compositions adjacent to lamellar or corona garnet which are 11 to 15 mole % lower in An and approximately 1 mole % higher in Or compared to compositions far removed from garnet (Fig. 4). Representative microprobe analyses of plagioclase in mafic rocks are given in Table 4. The analyses in the central regions of grains have the best chance of representing the primary igneous compositions, and are in general somewhat more sodic than anorthositic plagioclases, as would be expected for later differentiates. However, the effects of the garnet-producing reactions on plagioclase compositions in these rocks makes determination of plagioclase fractionation trends by direct measurement rather difficult.

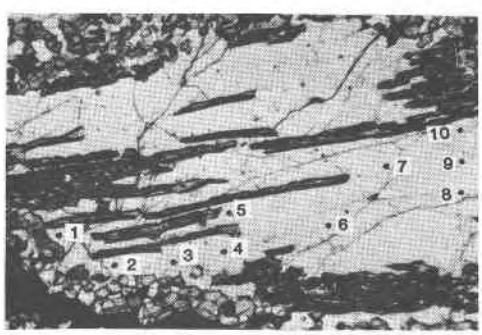

	1	2	3	4	5	6	7	8	9	10
Ab	76.8	72.9	70.4	63.7	70.2	64.0	61.5	61.5	61.9	72.1
An	20.7	25.0	27.8	34.6	27.4	34.2	36.6	36.7	36.3	25.2
Or	2.5	2.1	1.8	1.7	2.4	1.8	1.9	1.8	1.8	2.7

Fig. 4 Photomicrograph illustrating variability of plagioclase (white) composition (mole %) in relation to lamellar or coronitic garnet (dark, high relief). Sample MM-6. Length of photograph is approximately 6 mm.

Fe–Ti oxides

Fe–Ti oxide minerals are a ubiquitous constituent of anorthosite suite rocks, and are present in major proportions in the mafic rocks and associated ore deposits. Like the pyroxenes, the oxides exhibit complex subsolidus exsolution features. However, in addition to exsolution in the strict sense (hematite lamellae in ilmenite, pleonaste lamellae in magnetite), textural and compositional relations among the Fe–Ti oxides may be further complicated to varying degrees by subsolidus oxidation–reduction reactions. This has produced, for example, ilmenite oxy-exsolution lamellae in magnetite. Both ED and WD microprobe techniques were used in analyzing the compositions of these Fe–Ti oxide minerals. For the ED analyses, a defocussed beam of up to 20 microns in diameter was used in an attempt to incorporate hematite lamellae in ilmenite and pleonaste lamellae in magnetite. No attempt was made to integrate oxy-exsolution lamellae, but in some cases these could not be avoided. Textural relations and ED compositions of Fe–Ti oxides are summarized in Table 5. Average ED compositions are plotted on a TiO_2–FeO–Fe_2O_3 diagram in Figure 5.

Primary igneous compositions of Fe–Ti oxides are rarely preserved in plutonic rocks because of the extensive degree to which coexisting titanomagnetite and ferrian ilmenite react upon cooling according to the equation

$$Hem_{ss} + Usp_{ss} = Mag_{ss} + Ilm_{ss}. \quad (1)$$

This results in oxidation of the ulvöspinel component in titanomagnetite and corresponding reduction of the hematite component in ferrian ilmenite, forming ilmenite and magnetite, respectively, either

Table 4. Representative wavelength dispersive microprobe analyses of plagioclases

	SA-3A		SA-5		5683d		MM-6**		SR-9	
	core	rim	core	rim	core	rim	core	rim	core	rim
SiO_2	56.05	60.17	55.72	56.89	58.77	60.77	58.92	61.88	59.70	62.20
TiO_2	0.00	0.00	0.04	0.01	0.00	0.00	0.00	0.04	0.00	0.02
Al_2O_3	27.79	25.59	27.77	26.88	26.27	24.63	26.29	24.28	25.01	24.21
FeO*	0.39	0.24	0.11	0.16	0.06	0.14	0.12	0.13	0.01	0.15
MgO	0.06	0.00	0.00	0.00	0.00	0.00	0.00	0.00	0.00	0.00
CaO	8.77	6.59	9.60	8.33	7.76	5.88	7.55	5.29	6.38	5.09
Na_2O	6.00	7.60	5.69	6.15	7.17	8.28	7.01	8.37	7.64	8.61
K_2O	0.57	0.59	0.56	0.62	0.38	0.29	0.33	0.47	0.34	0.42
Total	99.63	100.78	99.49	99.04	100.41	99.99	100.22	100.46	99.08	100.70
Structural Formula based on 8 oxygens										
Si	2.530	2.665	2.521	2.575	2.618	2.705	2.625	2.736	2.682	2.742
Al	1.479 / 4.009	1.336 / 4.001	1.481 / 4.002	1.434 / 4.009	1.380 / 3.998	1.293 / 3.998	1.381 / 4.006	1.266 / 4.002	1.324 / 4.006	1.258 / 4.000
Ti	-	-	0.001	-	-	-	-	0.001	-	0.001
Fe*	0.015	0.009	0.004	0.006	0.002	0.005	0.005	0.005	-	0.006
Mg	0.004	-	-	-	-	-	-	-	-	-
Ca	0.424	0.313	0.465	0.404	0.370	0.280	0.360	0.250	0.307	0.241
Na	0.525	0.653	0.499	0.540	0.619	0.715	0.606	0.718	0.665	0.736
K	0.033 / 1.001	0.033 / 1.008	0.032 / 1.001	0.036 / 0.986	0.021 / 1.012	0.017 / 1.017	0.019 / 0.990	0.027 / 1.001	0.019 / 0.991	0.024 / 1.008
Ab	53.5	65.4	50.1	55.1	61.3	70.6	61.5	72.1	67.1	73.6
An	43.2	31.3	46.7	41.2	36.6	27.7	36.6	25.2	31.0	24.0
Or	3.3	3.3	3.2	3.7	2.1	1.7	1.9	2.7	1.9	2.4

* Total Fe as FeO; ** See Fig. 4

as discrete grains (external granule "exsolution") or as thin lamellae in the host grains (Buddington and Lindsley, 1964). The overall result is an increase in the ilmenite and magnetite components of the rhombohedral and spinel series phases, respectively, causing a counterclockwise rotation of their tie-lines on the TiO_2–FeO–Fe_2O_3 diagram.

While hematite lamellae in ilmenite and pleonaste lamellae in magnetite were incorporated in the defocussed beam ED microprobe analyses, oxy-exsolution lamellae in magnetite and magnetite reduction-exsolution lamellae in ilmenite were avoided, and as a result, many of the compositions of coexisting Fe–Ti oxides shown in Figure 5 represent those which resulted after subsolidus reconstitution. Attempts to re-integrate the oxidation or reduction lamellae to obtain primary compositions would not be possible because of the unknown extent of previous external granule "exsolution" (Buddington and Lindsley, 1964).

Despite the effects of subsolidus recrystallization, there is a perceptible compositional trend among the Fe–Ti oxide minerals. In the anorthosites and other early cumulates, ilmenites tend to be richer in hematite component, and coexisting spinels richer in magnetite component, compared to the oxides in later cumulates and mafic gabbro dikes. Similar relationships in other anorthosite massifs (Hargraves, 1962; Anderson, 1966; Duchesne, 1972) have been interpreted as an indication of progressive reduction of the melts during differentiation. However, because of the effects of counter-clockwise rotation of Fe–Ti oxide tie lines in response to reaction (1) during cooling, as previously discussed, rocks whose bulk oxide assemblage is dominated by ilmenite [ilm/(ilm + mag) $\geq$ 0.9] will tend to retain near-primary ilmenite compositions, but magnetite compositions will be widely different (much more Ti-poor) than primary values. Conversely, magnetite-rich rocks [ilm/(ilm + mag) $\leq$ 0.75] will contain

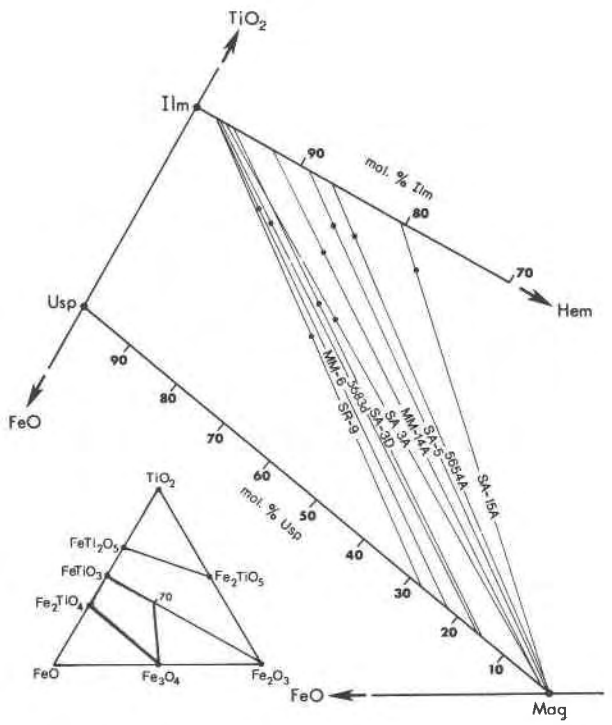

Fig. 5 Average ED microprobe compositions of Fe–Ti oxide minerals from the Marcy massif plotted in terms of TiO_2–FeO–Fe_2O_3. Dots represent bulk compositions of oxide assemblages given from modes. Enlarged area represents shaded area in inset.

magnetites with compositions closer to primary values than coexisting ilmenites. This relationship is supported by the distinct correlation between Fe–Ti oxide compositions and the modal proportions of ilmenite and magnetite (Table 5, Fig. 5). The geothermometer–oxygen barometer of Buddington and Lindsley (1964) thus cannot be used to obtain estimates of primary temperature and fO_2.

WD microprobe analyses of coexisting Fe–Ti oxides from a layered cumulate sequence which is gradational upwards from a basal oxide-rich pyroxenite to leuconorite are given in Table 6. There is a slight but progressive increase in hematite component in ilmenite and a decrease in ulvöspinel component in magnetite stratigraphically upward in this sequence, but these may not reflect primary variations, as discussed above. However, minor elements may be used as reliable indicators of primary fractionation trends (Himmelberg and Ford, 1977). Both magnetites and ilmenites from this sequence show a progressive decrease in Al_2O_3, MnO, and MgO, and a progressive increase in Cr_2O_3 and V_2O_3 with stratigraphic height. Noteworthy is the nearly threefold increase in V_2O_3 among magnetites, to a maximum of 3.0 wt.% in sample SA-5 (Table 6).

Discussion

The mafic cumulates and dikes of the Marcy massif are interpreted as late-stage differentiates from a magma that had undergone extensive fractionation of plagioclase, followed sequentially by crystallization and accumulation of pyroxenes, Fe–Ti oxides, apatite, and Fe-rich olivine. Crosby (1968) and Buddington (1969) have proposed flow differentiation models by which plagioclase crystals migrated to the central regions of ascending magmas, to form a core zone of relatively pure, coarse-grained anorthosite. The liquid in the outer regions became progressively enriched in mafic constitutents, and subsequently crystallized as a somewhat finer-grained sheath of more mafic material. Local incorporation of earlier-formed plagioclase accumulations by this mafic-enriched liquid could account for the block structures common in most anorthosite massifs (Isachsen, 1969). Although flow differentiation appears to be a satisfactory mechanism to account for the formation of the pure anorthosites and their restriction to the central regions of the massifs, the nature of the conformable mafic–ultramafic layers described here suggests that they were formed by gravitational accumulation. It is suggested here that differentiation by gravitational means became the dominant mechanism subsequent to emplacement of the partially solidified melts. In the case of the Marcy massif, final emplacement is inferred to have taken place at a stage in the crystallization history at least as early as the time when the pyroxenes first precipitated, allowing the formation of the early, Mg-rich ultramafic cumulates in a relatively static environment. The occurrence of the mafic facies in the border zones of the massif, and hence structurally above the earlier-formed anorthosites of the core zone, could be interpreted as evidence that plagioclase sank, at least in the early stages of crystallization.

The relatively minor volume of mafic rocks compared to the associated anorthosites is consistent with a rather feldspathic parental magma composition, possibly in the gabbroic anorthosite (77.5–90% normative plagioclase) range. The exact composition of the parental magma is difficult to determine because an accurate field estimation of the volume of mafic rich rock is not possible. Although highly aluminous magmas such as gabbroic anorthosite

Table 5. Microtextures and compositions (EDA) of coexisting Fe–Ti oxides

Sample No.	Rock Type	Modal Compositions Ilm+Mag	Ilm/(Ilm+Mag)	Microtextures	Compositional Range	Average Comp.	No. of Analyses
CUMULATES:							
5654A	Anorthosite	1.5	0.90	Ilm: coarse hem. lamellae Mag: homogeneous	$Hem_{10.4 - 15.6}$	$Hem_{13.3}$ $Usp_{0.0}$	7 6
SL-11Y	Oxide rich pyroxenite	23.1	0.82	Ilm: coarse hem. lamellae, depleted near mag. Mag: homogeneous	$Hem_{11.1 - 17.0}$ $Usp_{0.0 - 0.5}$	$Hem_{14.5}$ $Usp_{0.2}$	4 8
SL-11A	Leuconorite	4.5	0.90	Ilm: coarse hem lamellae, depleted near mag. Mag: homogeneous	$Hem_{9.8 - 16.2}$ $Usp_{0.0 - 0.3}$	$Hem_{12.5}$ $Usp_{0.1}$	6 6
SA-3D	Oxide rich pyroxenite	39.5	0.65	Ilm: homogeneous Mag: 3 sets of pleonaste lamellae, discrete pleonaste	$Hem_{2.9-4.0}$ $Usp_{13.8 - 14.9}$	$Hem_{3.5}$ $Usp_{14.5}$	3 3
SA-3A	Leuconorite	1.7	0.65	Ilm: homogeneous Mag: few pleonaste lamellae, few ilm oxid. lamellae	$Hem_{2.1 - 4.7}$ $Usp_{0.6 - 4.0}$	$Hem_{2.9}$ $Usp_{1.9}$	6 5
SA-5	Leuconorite	1.0	0.90	Ilm: fine hem. lamellae, depleted near mag. Mag: homogeneous	$Hem_{8.3 - 12.4}$ $Usp_{0.0 - 3.0}$	$Hem_{10.9}$ $Usp_{0.8}$	9 9
MM-56B	Oxide rich mafic gabbro	16.3	0.94	Ilm: coarse hem. lamellae, depleted near mag. Mag: few tiny pleonaste lamellae	$Hem_{13.2 - 18.2}$ $Usp_{0.3 - 1.5}$	$Hem_{15.5}$ $Usp_{1.1}$	6 6
SA-15A	Oxide rich gabbro	13.6	0.90	Ilm: coarse hem lamellae, depleted near mag. Mag: fine pleonaste lamellae	$Hem_{17.9 - 20.9}$ $Usp_{0.0 - 0.8}$	$Hem_{19.6}$ $Usp_{0.1}$	3 8
5683d	Oxide rich mafic troctolite	11.7	0.72	Ilm: homogeneous Mag: 2 sets of tiny pleonaste lamellae, abundant ilm oxid. lamellae	$Hem_{1.1 - 3.2}$ $Usp_{10.0 - 21.5}$	$Hem_{2.4}$ $Usp_{15.7}$	3 14
DIKES:							
MM-14A	Oxide rich mafic norite	13.5	0.81	Ilm: homogeneous Mag: fine pleonaste lamellae	$Hem_{5.8 - 9.1}$ $Usp_{0.2 - 1.5}$	$Hem_{7.5}$ $Usp_{0.8}$	9 12
MM-6	Oxide rich mafic gabbro	14.0	0.72	Ilm: homogeneous Mag: few pleonaste lamellae, few ilm oxid. lamellae	$Hem_{1.0 - 2.6}$ $Usp_{21.4 - 22.3}$	$Hem_{1.8}$ $Usp_{22.0}$	2 3
SR-9	Oxide rich gabbro	12.6	0.54	Ilm: homogeneous Mag: few pleonaste lamellae	$Hem_{0.8 - 2.4}$ $Usp_{26.8 - 27.7}$	$Hem_{1.8}$ $Usp_{27.1}$	4 3

have been suggested as much as forty years ago (Buddington, 1939), their existence has been questioned and their possible modes of origin have been debated. The recent discovery of sills and dikes of gabbroic anorthosite composition provides the first direct evidence for the existence of these magmas (Crosby, 1969; Husch *et al.*, 1975; Isachsen *et al.*, 1975; Simmons, *et al.*, 1980; Wiebe, 1979), although their origin remains somewhat of a problem. Emslie (1978) has proposed that the aluminous magmas which gave rise to massif-type anorthosites were produced by high-pressure fractionation of olivine and orthopyroxene from mantle-derived olivine tholeiite magmas which accumulated near the base of the continental crust. The aluminous melts were then emplaced into higher levels in the crust, where they precipitated only plagioclase at the liquidus. This model accounts for the relatively high fe* of the anorthositic rocks (Emslie, 1973; Simmons and Hanson, 1978), and is consistent with recent Sm–Nd isotope studies of the Adirondack Marcy massif which indicate an ultramafic source area for the

Table 6. Representative WD microprobe analyses of Fe–Ti oxides

	Magnetites			Ilmenites		
	SA-3D	SA-3A	SA-5	SA-3D	SA-3A	SA-5
SiO_2	0.03	0.07	0.05	0.02	0.01	0.01
TiO_2	3.34	0.67	0.05	52.61	50.92	47.86
Al_2O_3	1.51	0.67	0.54	0.06	0.04	0.03
Cr_2O_3	0.37	1.16	3.84	0.01	0.03	0.15
Fe_2O_3	58.15	61.83	61.12	2.22	3.03	8.34
FeO	33.65	30.88	31.31	42.77	42.23	41.11
MnO	0.07	0.02	0.01	0.46	0.27	0.26
MgO	0.18	0.07	0.01	2.30	1.85	0.94
V_2O_3*	1.18	2.10	3.00	0.13	0.22	0.59
Total	98.48	97.47	99.93	100.58	98.60	99.29
Structural formula based on 3 cations (magnetite) or 2 cations (ilmenite)						
Si	0.001	0.003	0.002	0.000	0.000	0.000
Ti	0.097	0.020	0.001	0.977	0.968	0.912
Al	0.069	0.031	0.024	0.002	0.001	0.001
Cr	0.011	0.036	0.116	0.000	0.001	0.003
Fe^{3+}	1.689	1.825	1.761	0.041	0.058	0.159
Fe^{2+}	1.085	1.014	1.003	0.882	0.892	0.871
Mn	0.002	0.001	0.000	0.010	0.006	0.006
Mg	0.010	0.004	0.001	0.085	0.070	0.036
V	0.036	0.066	0.092	0.003	0.004	0.012
	3.000	3.000	3.000	2.000	2.000	2.000
Mag (Ilm)	89.70	97.88	99.84	(97.71)	(96.87)	(91.63)
Usp (Hem)	10.30	2.12	0.16	(2.29)	(3.13)	(8.37)

*V_2O_3 abundances were corrected for TiK_β overlap by subtracting an empirically determined 1% of TiK_α counts from VK_α counts prior to further matrix corrections.

melts parental to the anorthosites and related mafic differentiates (Ashwal *et al.*, 1980).

Acknowledgments

This study was done in partial fulfillment of the requirements for the degree of Doctor of Philosophy at Princeton University. Financial support came from NASA Grant NGL-31-001-283, Lincoln S. Hollister, principal investigator, and from the Department of Geological and Geophysical Sciences, Princeton University. Some of the data were collected while the author held a National Research Council Resident Research Associateship at NASA/Johnson Space Center. A portion of the research reported in this paper was done while the author was a Resident Research Scientist at the Lunar and Planetary Institute, which is operated by the Universities Space Research Association under Contract No. NASW–3389 with the National Aeronautics and Space Administration. The manuscript was critically reviewed by R. B. Hargraves, E. Dowty, G. Ryder, J. L. Warner, R. F. Emslie, and S. R. Bohlen. Assistance in the field was provided by F. B. Nimick, R. Warren, and M. A. Arthur. Maps were provided by Y. W. Isachsen and P. R. Whitney of the New York State Museum and Science Service. C. G. Kulick, R. W. Brown and D. W. Phelps provided assistance with the electron microprobes. This is L.P.I. Contribution No. 447.

References

Anderson, A. T., Jr. (1966) Mineralogy of the Labrieville anorthosite, Quebec. American Mineralogist 51, 1671–1711.

Anderson, A. T., Jr. (1969) Massif type anorthosite: a widespread Precambrian igneous rock. In Origin of Anorthosite and Related Rocks, Y. W. Isachsen, ed., New York State Museum and Science Service Memoir 18, 47–55, N. Y.

Ashwal, L. D. (1978a) Crystallization history of massif-type anorthosite (abstract). EOS: Transactions of the American Geophysical Union 59, 393.

Ashwal, L. D. (1978b) Petrogenesis of massif-type anorthosites: crystallization history and liquid line of descent of the Adirondack and Morin complexes. Ph.D. thesis, Princeton University, 136 pp.

Ashwal, L. D. and Seifert, K. E. (1980) Rare earth element geochemistry of anorthosite and related rocks from the Adirondacks, New York, and other massif-type complexes. Bulletin of the Geological Society of America 91, 105–107, 659–684.

Ashwal, L. D., Wooden, J. L. and Shih, C. -Y. (1980) Nd and Sr isotope geochronology of the Marcy anorthosite massif, Adirondacks, New York (abstract). Geological Society of America Abstracts with Programs, 12, 380.

Bohlen, S. R. and Essene, E. J. (1978) Igneous pyroxenes from metamorphosed anorthosite massifs. Contributions to Mineralogy and Petrology 65, 433–442.

Buddington, A. F. (1939) Adirondack igneous rocks and their metamorphism. Geological Society of America Memoir 18, 343 pp.

Buddington, A. F. (1953) Geology of the Saranac Quadrangle, New York. New York State Museum Bulletin 346, 100 pp.

Buddington, A. F. (1960) The origin of anorthosite reevaluated. Records Geological Survey of India 86, Part 3, 421–432.

Buddington, A. F. (1969) Adirondack anorthosite series. In Y. W. Isachsen, ed., Origin of Anorthosite and Related Rocks, New York State Museum and Science Service, Memoir 18, 215–231.

Buddington, A. F. and Lindsley, D. L. (1964) Iron titanium oxide minerals and synthetic equivalents. Journal of Petrology 5, 310–357.

Crosby, P. (1968) Igneous differentiation of the Adirondack anorthosite series. XXXIII International Geological Congress 2, 31–48.

Crosby, P. (1969) Petrogenetic and statistical implications of modal studies in Adirondack anorthosite. In Y. W. Isachsen, ed., Origin of Anorthosite and Related Rocks, New York State Museum and Science Service Memoir 18, 289–303.

Davis, B. T. C. (1971) Bedrock geology of the St. Regis Quadrangle, New York. New York State Museum and Science Service, Map and Chart Series Number 16, 34 pp.

deWaard, D. (1965) A proposed subdivision of the granulite facies. American Journal of Science 263, 455–461.

deWaard, D. (1970) The anorthosite-charnockite suite of rocks of Roaring Brook valley in the Eastern Adirondacks (Marcy Massif). American Mineralogist 55, 2063–2075.

Duchesne, J.-C. (1972) Iron-titanium oxide minerals in the Bjerkrem-Sogndal massif, southwestern Norway. Journal of Petrology 13, 57–81.

Emslie, R. F. (1973) Some chemical characteristics of anorthosite suites and their significance. Canadian Journal of Earth Sciences 10, 54–71.

Emslie, R. F. (1975) Nature and origin of anorthositic suites. Geoscience Canada 2, 99–104.

Emslie, R. F. (1978) Anorthosite massifs, rapakivi granites, and late Proterozoic rifting of North America. Precambrian Research 7, 61–98.

Green, T. H., Brunfelt, A. O. and Heier, K. S. (1969) Rare earth element distribution in anorthosite and associated high grade metamorphic rocks, Lofoten-Vesteraalen, Norway. Earth and Planetary Science Letters 7, 93–98.

Green, T. H., Brunfelt, A. O. and Heier, K. S. (1972) Rare earth element distribution and K/Rb ratios in granulites, mangerites, and anorthosites, Lofoten-Vesteraalen, Norway. Geochimica et Cosmochimica Acta 36, 241–257.

Gross, S. O. (1968) Titaniferous ores of the Lake Sanford district, New York. In J. D. Ridge, ed., Ore Deposits of the United States, American Institute of Mining, Metallurgical, and Petroleum Engineers, N. Y., 140–154.

Hargraves, R. B. (1962) Petrology of the Allard Lake anorthosite suite, Quebec. In, Petrologic Studies, Geological Society of America Buddington Volume, 163–189.

Himmelberg, G. R. and Ford, A. B. (1977) Iron-titanium oxides of the Dufek intrusion, Antarctica. American Mineralogist 62, 623–633.

Husch, J. M., Kleinspehn, K. and McLelland, J . (1975) Anorthositic rocks in the southern Adirondacks: basement or non-basement? Geological Society of America Abstracts with Programs 7, 78.

Isachsen, Y. W., McLelland, J. and Whitney, P. R. (1975) Anorthosite contact relationships in the Adirondacks and their implications for geologic history. Geological Society of America Abstracts with Programs 7, 78.

Isachsen, Y. W. and Fisher, D. W. (1970) Geologic map of New York, Adirondack Sheet. University of the State of New York, The State Education Department, Albany, N. Y.

Isachsen, Y. (1969) Origin of anorthosite and related rocks—a summarization. In, Y. W. Isachsen, ed., Origin of Anorthosite and Related Rocks, New York State Museum and Science Service Memoir 18, 435–445.

Isachsen, Y. W. and Moxham, R. L. (1969) Chemical variation in plagioclase megacrysts from two vertical sections in the main Adirondack metanorthosite massif. In, Y. W. Isachsen, ed., Origin of Anorthosite and Related Rocks, New York State Museum and Science Service, Memoir 18, 255–265.

Jaffe, H. W., Robinson, P. and Tracy, R. J. (1975) Orientation of pigeonite exsolution lamellae in metamorphic augite: correlation with composition and calculated optimal phase boundaries. American Mineralogist 60, 9–28.

Kretz, R. (1963) Distribution of magnesium and iron between orthopyroxene and calcic pyroxene in natural mineral assemblages. Journal of Geology 71, 773–785.

Martignole, J. (1974) Mechanism of differentiation in the Morin anorthosite complex. Contributions to Mineralogy and Petrology 44, 99–107.

McLelland, J. M. and Whitney, P. R. (1977) The origin of garnet in the anorthosite-charnockite suite of the Adirondacks. Contributions of Mineralogy and Petrology 60, 161–181.

Morse, S. A. (1969) Layered intrusions and anorthosite genesis. In, Y. W. Isachsen, ed., Origin of Anorthosite and Related Rocks, New York State Museum and Science Service, Memoir 18, 175–187.

Morse, S. A. (1981) Kiglapait geochemistry III: potassium and rubidium. Geochimica et Cosmochimica Acta 45, 163–180.

Olmstead, J. F. (1969) Petrology of the Mineral Lake intrusion, northwestern Wisconsin. In, Y. W. Isachsen, ed., Origin of Anorthosite and Related Rocks, New York State Museum and Science Service Memoir 18, 149–161.

Philpotts, J. A., Schnetzler, C. C. and Thomas, H. H. (1966) Rare earth abundances in an anorthosite and a mangerite. Nature 212, 805–806.

Ranson, W. A. (1981) Anorthosites of diverse magma types in the Puttuaaluk Lake area, Nain complex, Labrador. Canadian Journal of Earth Sciences 18, 26–41.

Rose, E. R. (1969) Geology of titanium and titaniferous deposits of Canada. Geological Survey of Canada Economic Geology Report No. 25, 177 pp.

Ross, M. R. and Huebner, J. S. (1975) A pyroxene geothermometer based on composition-temperature relationships of naturally occurring orthopyroxene, pigeonite and augite. International Conference on Geothermometry and Geobarometry, Extended Abstracts, Pennsylvania State University, University Park, PA.

Seifert, K. E. (1978) Anorthosite-mangerite relations on Baker Mountain, New York, Bulletin of the Geological Society of America 89, 245–250.

Seifert, K. E., Voight, A. F., Smith, M. F., and Stensland, W. A. (1977) Rare earths in the Marcy and Morin anorthosite complexes. Canadian Journal of Earth Sciences 14, 1033–1045.

Sen, S. K. (1959) Potassium content of natural plagioclase and the origin of antiperthites. Journal of Geology 67, 479–495.

Simmons, E. C. and Hanson, G. N. (1978) Geochemistry and origin of massif-type anorthosites. Contributions of Mineralogy and Petrology 66, 119–135.

Simmons, E. C., Hanson, G. N. and Lumbers, S. B. (1980) Geochemistry of the Shawmere anorthosite complex, Kapuskasing structural zone, Ontario. Precambrian Research 11, 43–71.

Smith, J. V. (1975) Some chemical properties of feldspar. In, P. H. Ribbe, ed., Feldspar Mineralogy, Mineralogical Society of America Short Course Notes 2, SM-18—SM-29.

Streckeisen, A. (1976) To each plutonic rock its proper name. Earth Science Reviews 12, 1–33.

Subramaniam, A. P. (1956) Petrology of the anorthosite-gabbro mass at Kavadur, Madras, India. Geological Magazine 93, No. 4, 287–300.

Taylor, H. P., Jr., and Noble, J. A. (1969) Origin of magnetite in the zoned ultramafic complexes of southeastern Alaska. In, H. D. B. Wilson, ed., Magmatic Ore Deposits, Monograph 4, Economic Geology Publishing Co., 209–230.

Wager, R. L. and Brown, G. M. (1968) Layered Igneous Rocks, Oliver and Boyd, Ltd., Edinburgh, 588 pp.

Wiebe, R. A. (1979) Anorthositic dikes, southern Nain complex, Labrador. American Journal of Science 279, 394–410.

Manuscript received, January 9, 1981;
accepted for publication, August 31, 1981.